Efficient Data-Driven Modeling of Core Loss in Magnetic Materials for Power Electronics Systems: Supplementary Information

Junqi He[1,2,+], Siyang Li[1,2,+], Hao Sheng[1,2,3], Rui Gao[4], Ying Luo[1,2], Yiming Gai[1,2], Xudong Li[1,2], Yuyang Miao[1,2], Yutong Zhou[1,2], Yikang Xu[5], Tianjun He[5], Jian Huang[1,2,4,*]

[1]Hangzhou International Innovation Institute, Beihang University, Hangzhou, 311115, China

[2]Data Science and Intelligent Computing Laboratory, Beihang University, Hangzhou, 311115, Zhejiang, China

[3]School of Computer Science and Engineering, Beihang University, 100191, Beijing, China

[4]School of Software, Beihang University, 100191, Beijing, China

[5]Shanghai installation engineering group CO., LTD., Shanghai, 200080, China

*e-mail:hj@buaa.edu.cn

[+]These authors contributed equally to this work.

1. Dataset visualization

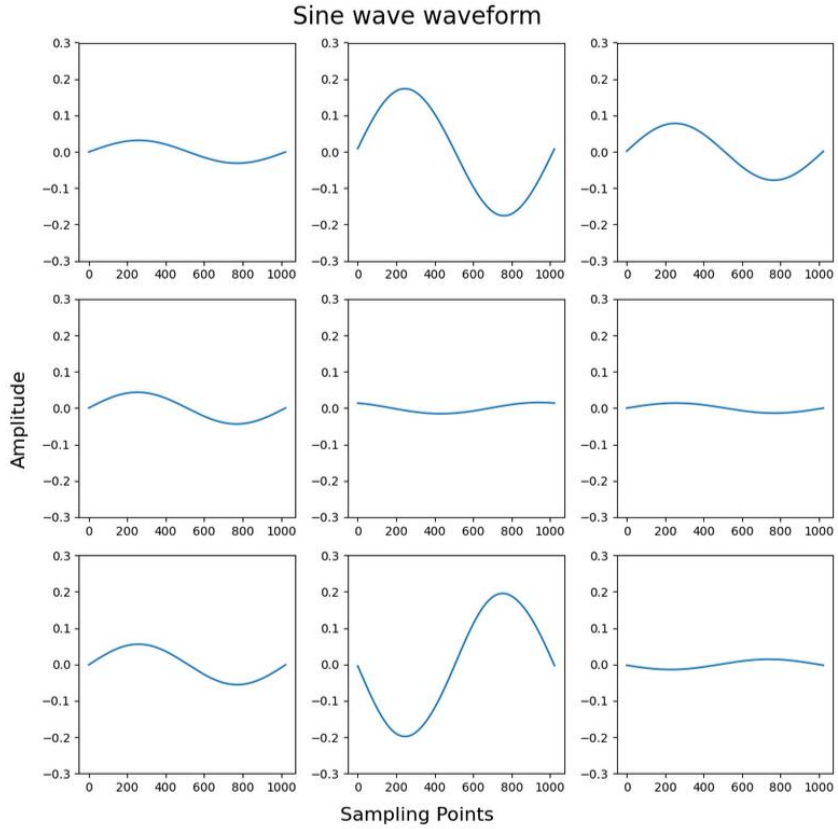

Fig. S1 Different sine waves.

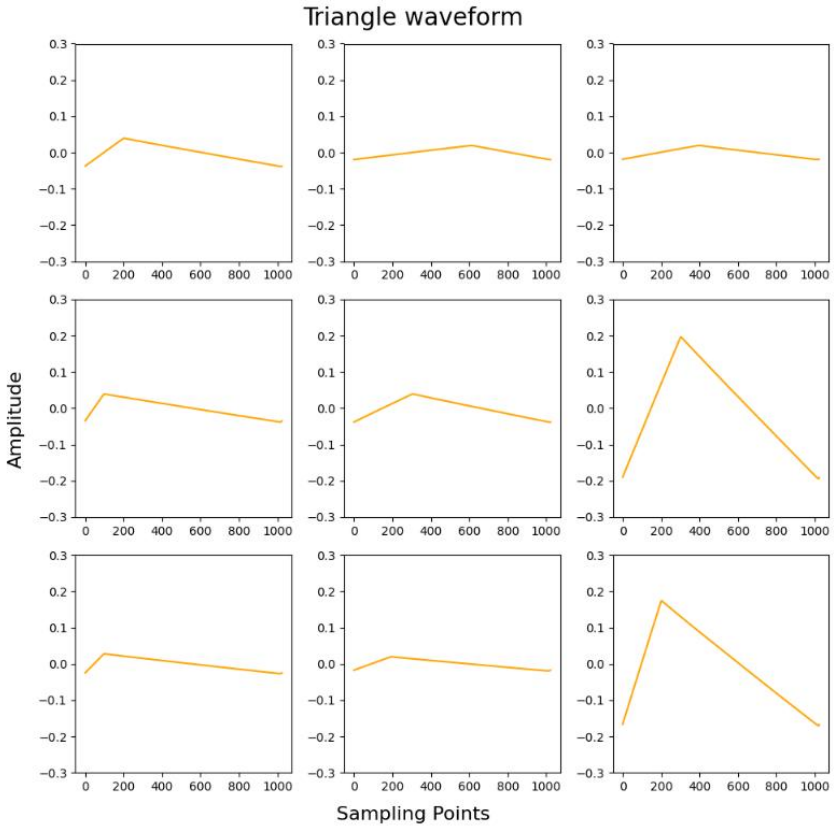

Fig. S2 Different triangle waves.

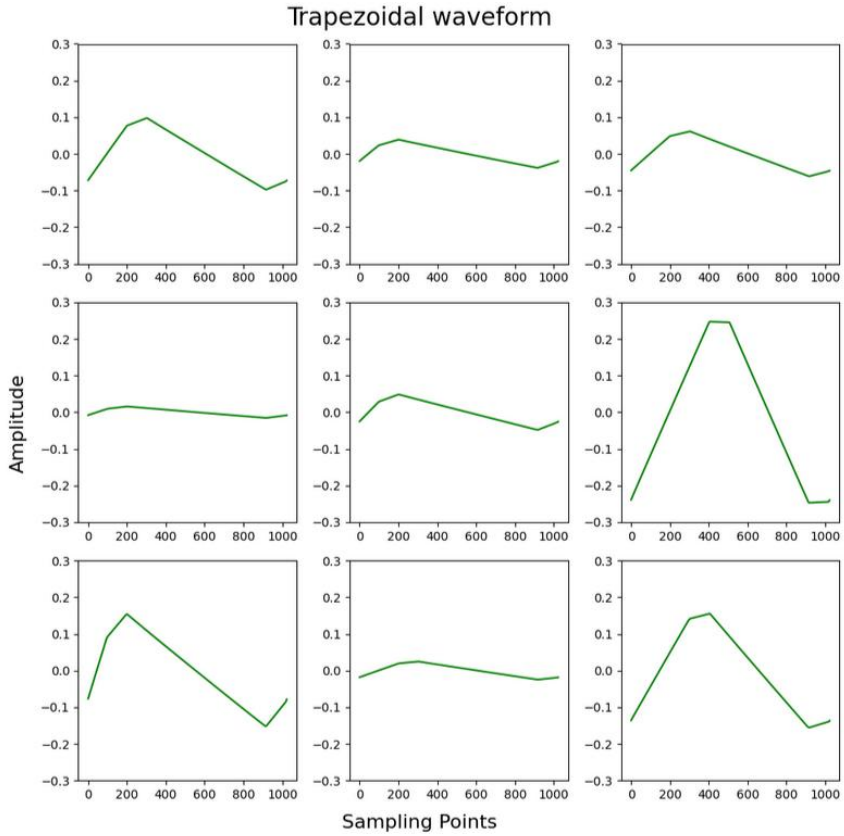

Fig. S3 Different trapezoidal waves.

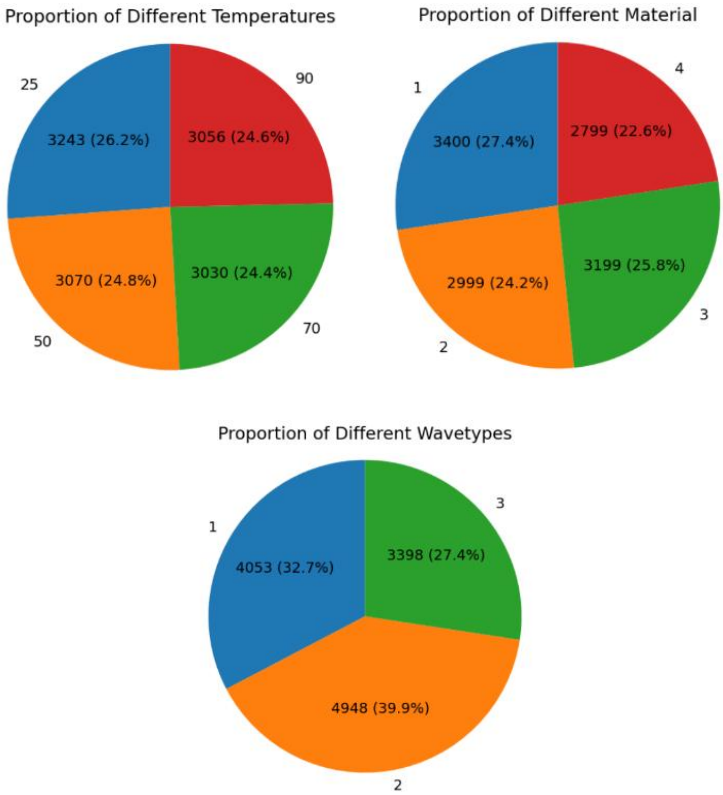

Fig. S4 Pie charts on temperature, material, and waveform (In the second pie chart, 1 represents 3C94, 2 represents 77, 3 represents N27, and 4 represents N87; In the third pie chart, 1 represents sine wave, 2 represents triangle wave, and 3 represents trapezoidal wave).

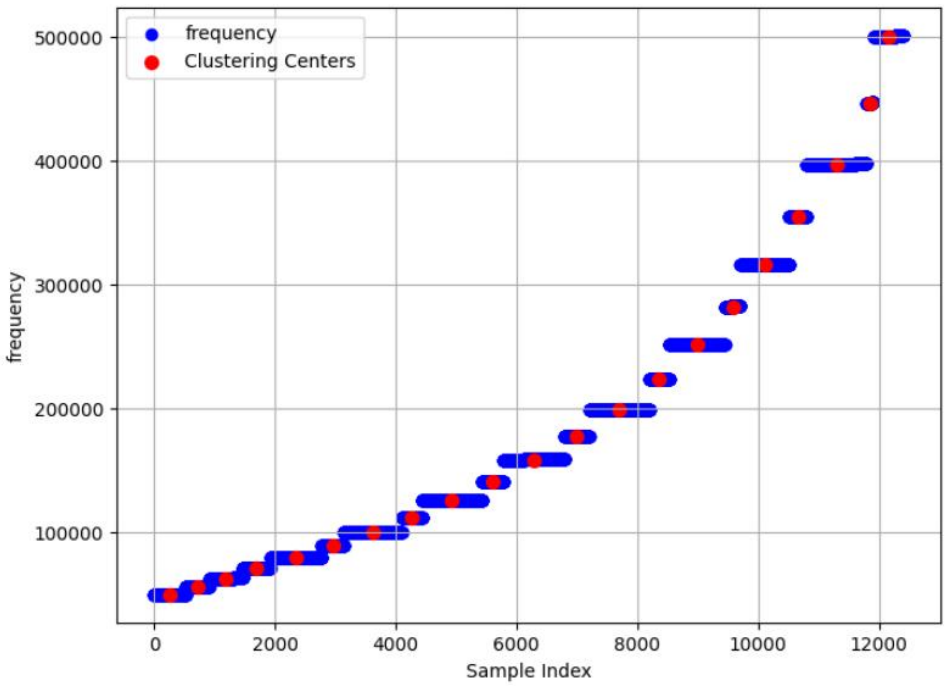

Fig. S5 Distribution diagram of different frequencies.

2. Steinmetz Equation fitting results

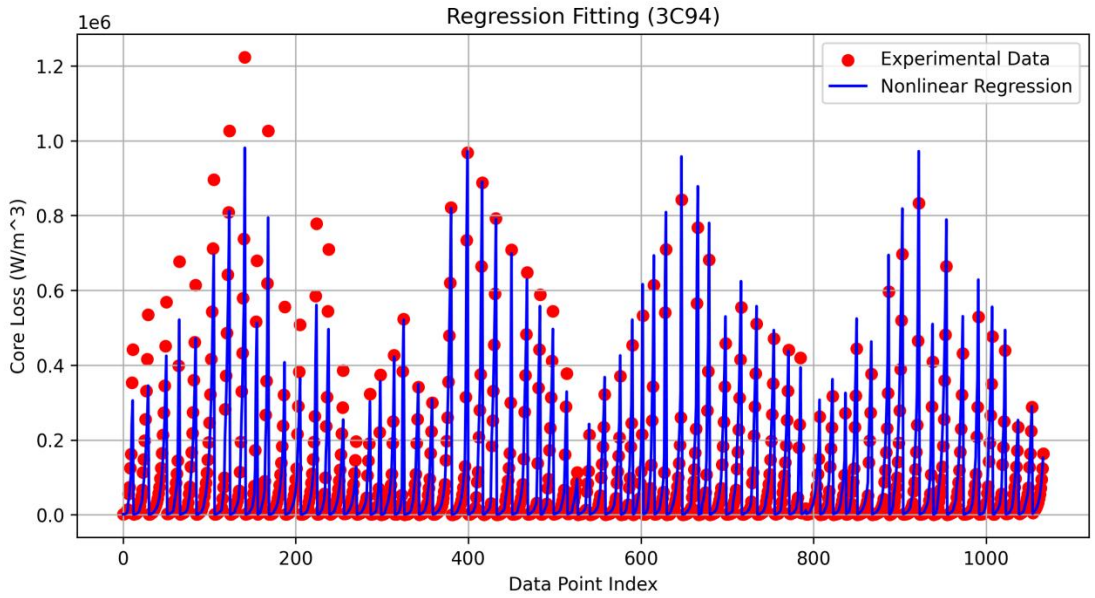

Fig. S6 Comparison between the fitting results of the SE and the actual values for 3C94.

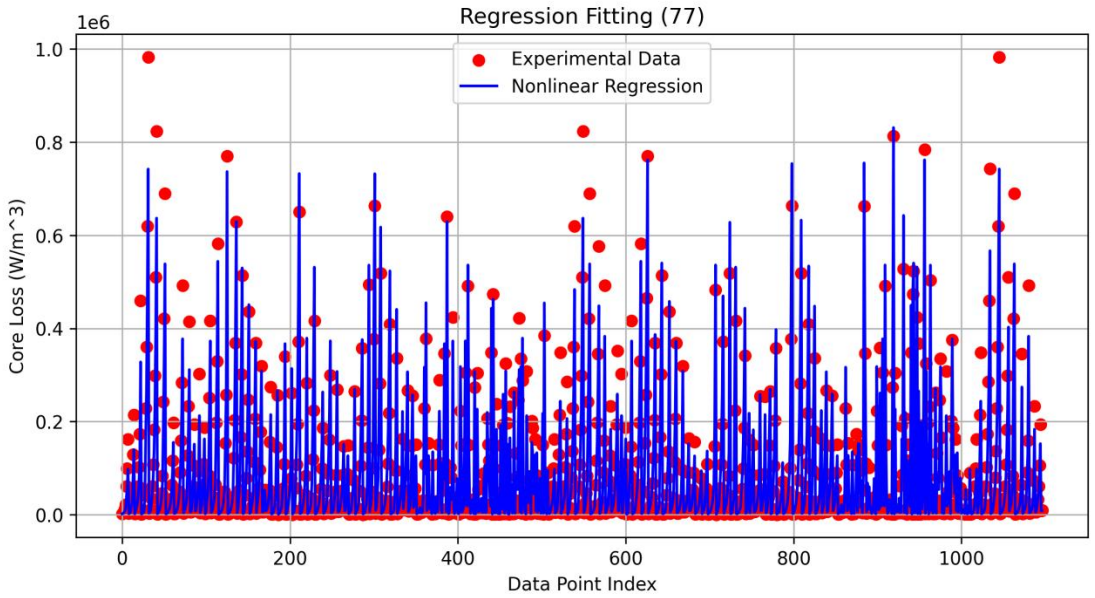

Fig. S7 Comparison between the fitting results of the SE and the actual values for 77.

Fig. S8 Comparison between the fitting results of the SE and the actual values for N27.

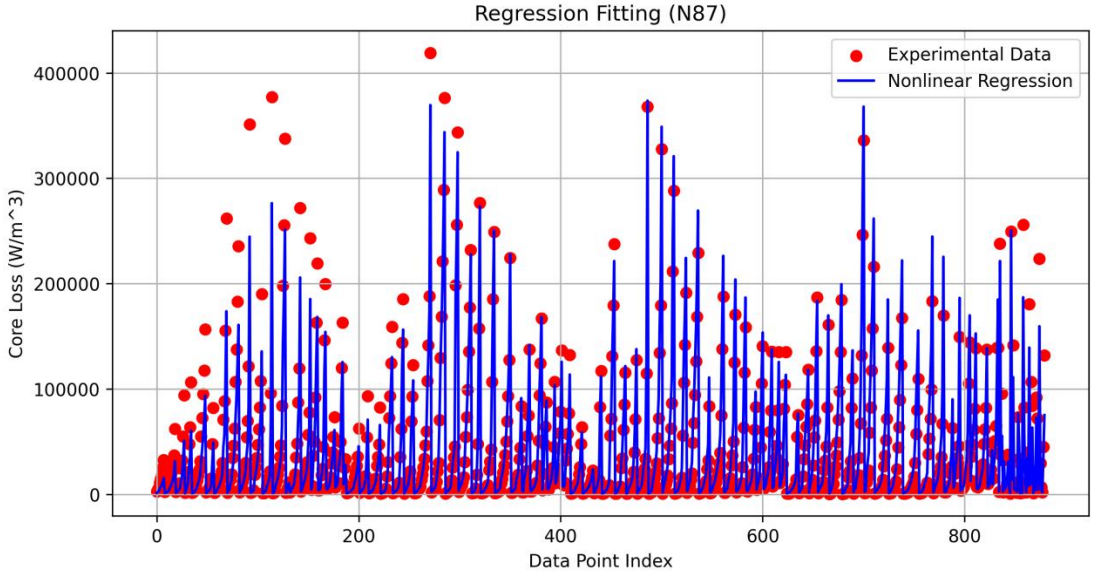

Fig. S9 Comparison between the fitting results of the SE and the actual values for N87.

3. Improved Generalized Steinmetz Equation fitting results

Tab. S1 IGSE training set fitting results

Material	$[k_1,\alpha_1,\beta_1]$	MSE	MAE	MAPE(%)	R^2
3C94	[0.024, 1.590, 2.204]	4602463142	34581.125	43.800	0.958
77	[0.042, 1.570, 2.224]	6269844974	41509.107	44.166	0.964
N27	[0.138, 1.430, 2.265]	6209107898	40541.740	38.024	0.972
N87	[0.306, 1.450, 2.266]	1920803175	22464.036	46.484	0.963

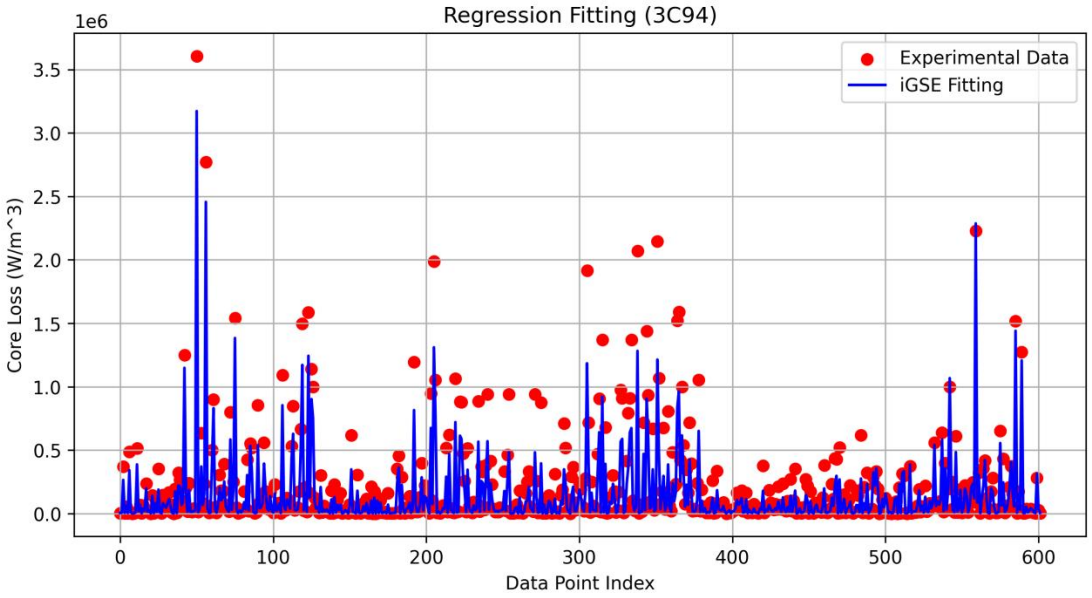

Fig. S10 Comparison between the fitting results of the iGSE and the actual values for 3C94.

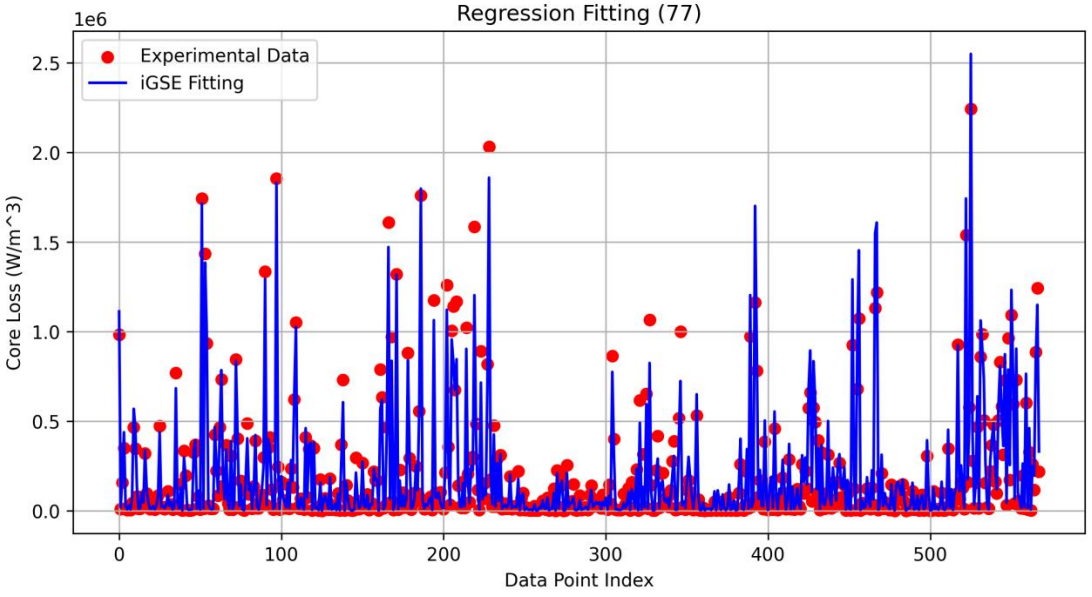

Fig. S11 Comparison between the fitting results of the iGSE and the actual values for 77.

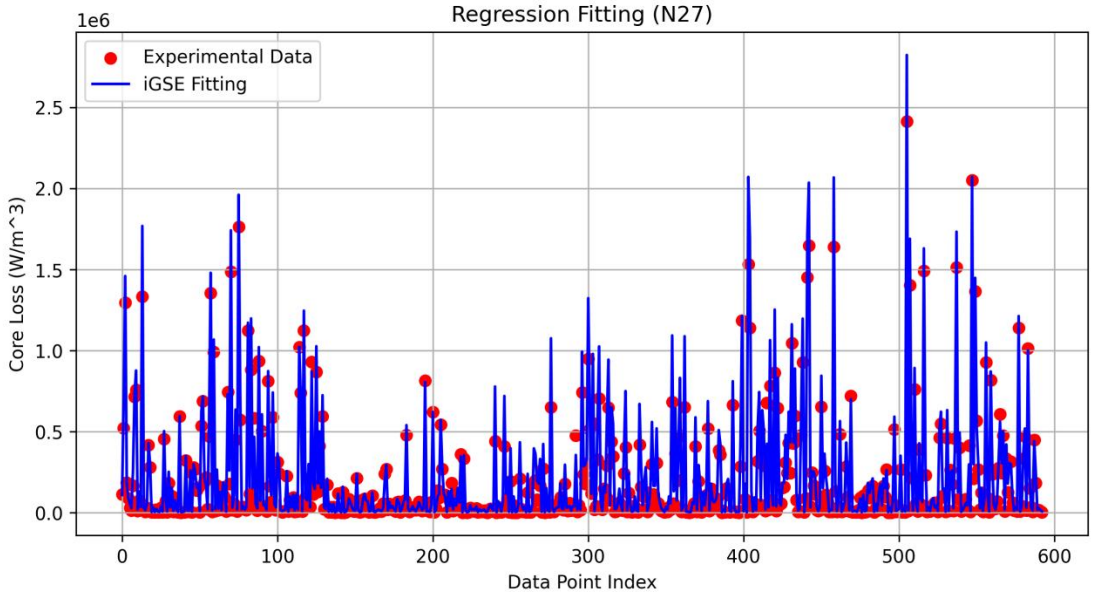

Fig. S12 Comparison between the fitting results of the iGSE and the actual values for N27.

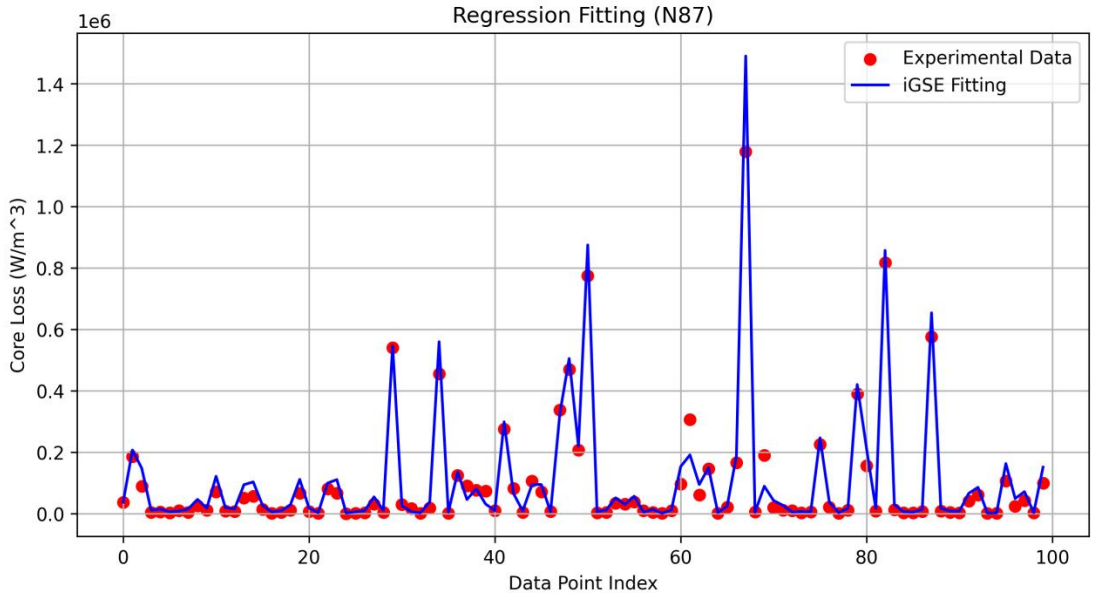

Fig. S13 Comparison between the fitting results of the iGSE and the actual values for N87.

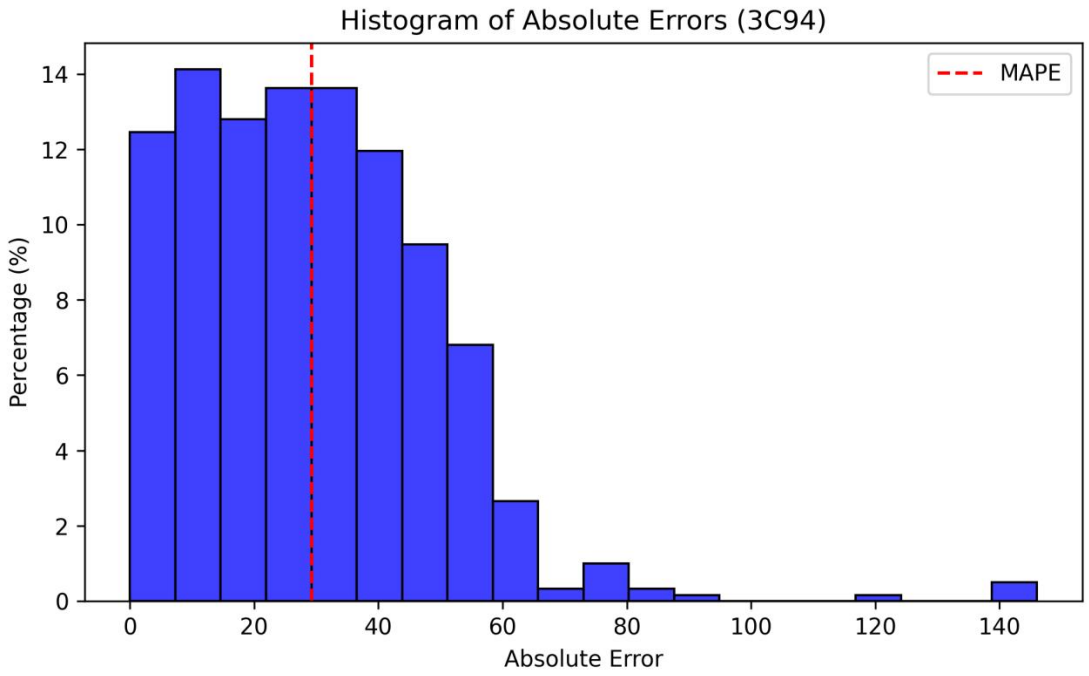

Fig. S14 Error histogram of iGSE fitting results for 3C94.

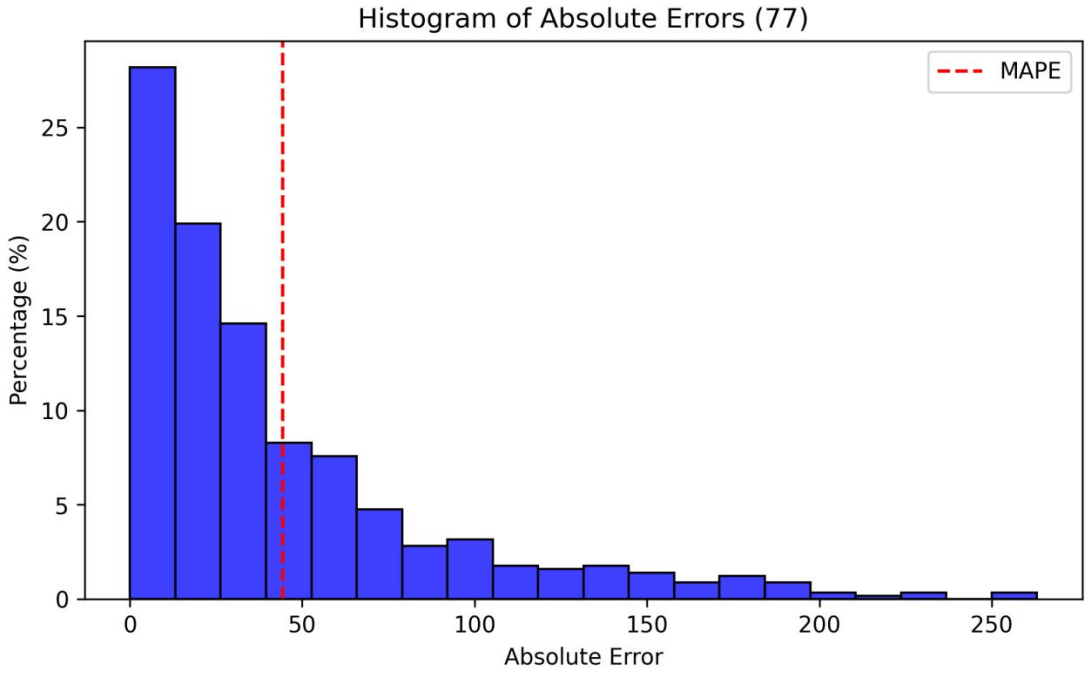

Fig. S15 Error histogram of iGSE fitting results for 77.

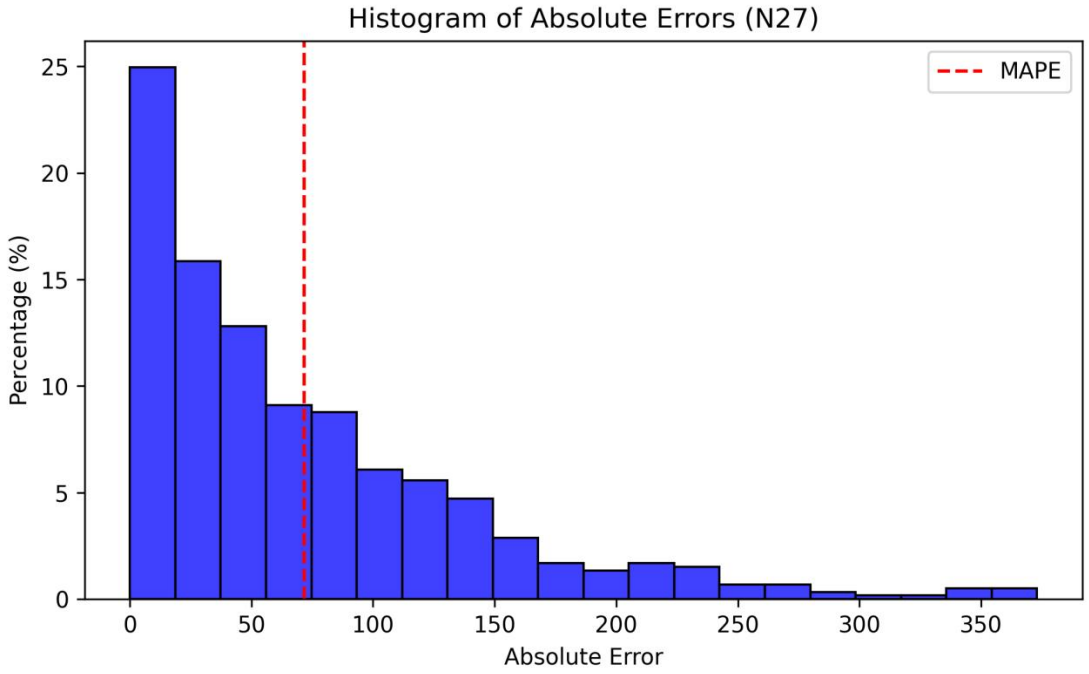

Fig. S16 Error histogram of iGSE fitting results for N27.

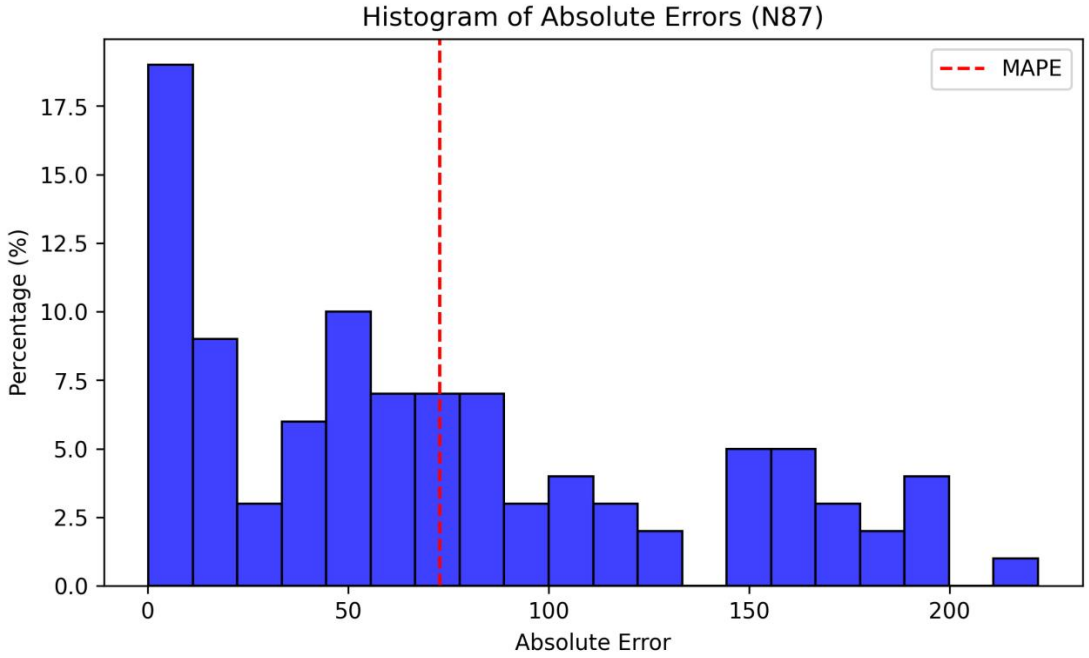

Fig. S17 Error histogram of iGSE fitting results for N87.

4. Feature extraction

The following 33 features were extracted from the magnetic flux density sequence:

1.Mean
2.Standard Deviation
3.Variance
4.Skewness
5.Kurtosis
6.Maximum Value
7.Minimum Value
8.Root Mean Square (RMS) Value
9.Peak-to-Peak Value
10.Zero-Crossing Rate
11.Spectral Centroid
12.Spectral Energy
13.Spectral Entropy
14.Spectral Peak at 1 Hz
15.Spectral Peak at 2 Hz
16.Spectral Peak at 3 Hz
17.Spectral Peak at 4 Hz
18.Spectral Peak at 5 Hz
19.Dominant Frequency
20.Spectral Bandwidth
21.Spectral Slope
22.Signal Power
23.Signal Smoothness
24.Low-Frequency Energy Ratio
25.Mid-Frequency Energy Ratio
26.High-Frequency Energy Ratio
27.Sum of Signal Values
28.Position of Maximum Flux Density Sequence
29.Position of Minimum Flux Density Sequence
30.First Quartile
31.Second Quartile (Median)
32.Third Quartile
33.Spectral Flatness

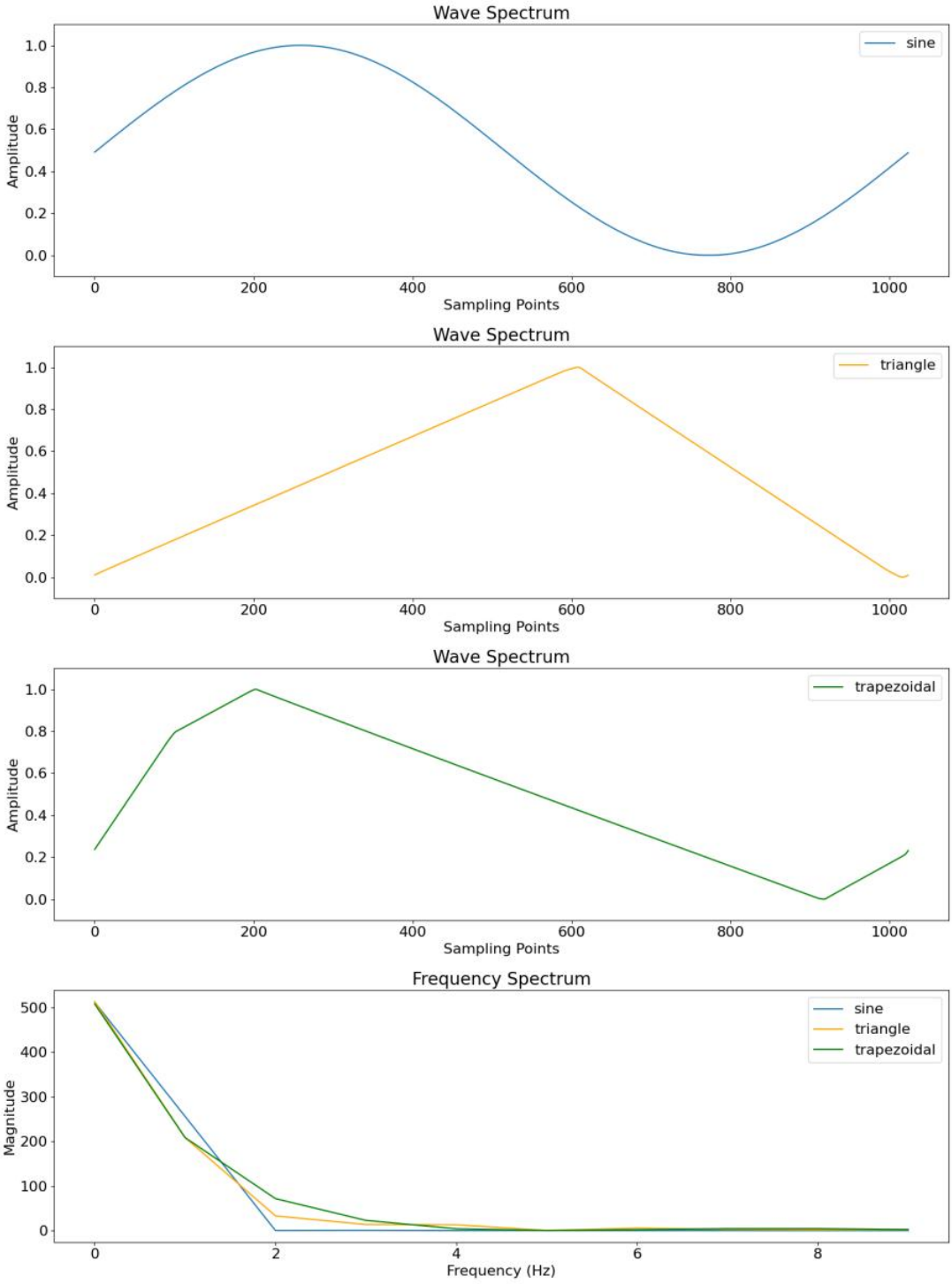

Fig. S18 Comparison of Time Domain and Frequency Domain Characteristics.

5. Prediction results of machine learning models

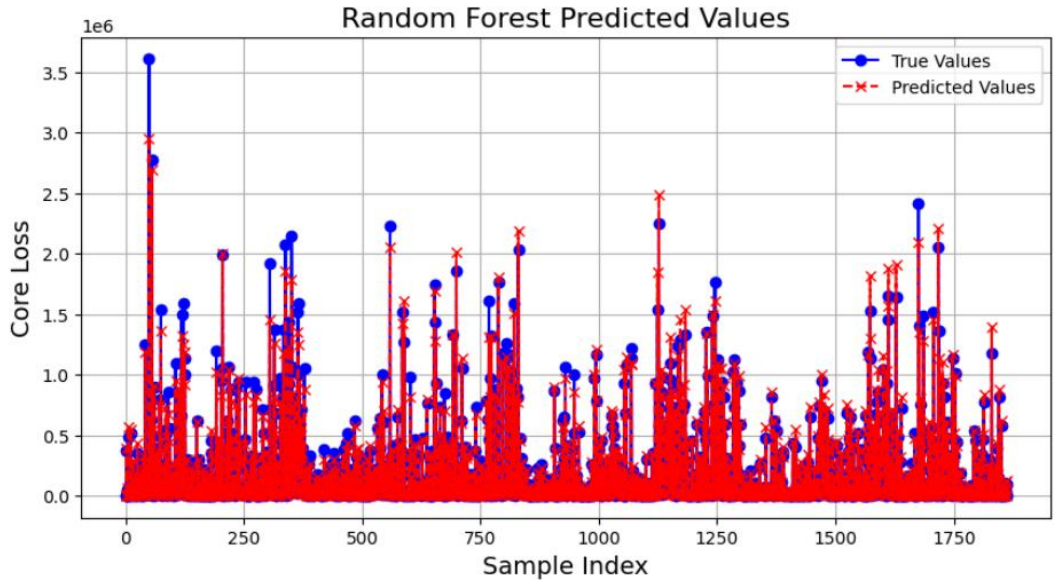

Fig. S19 Comparison between the predicted results of the Random Forest and the actual values.

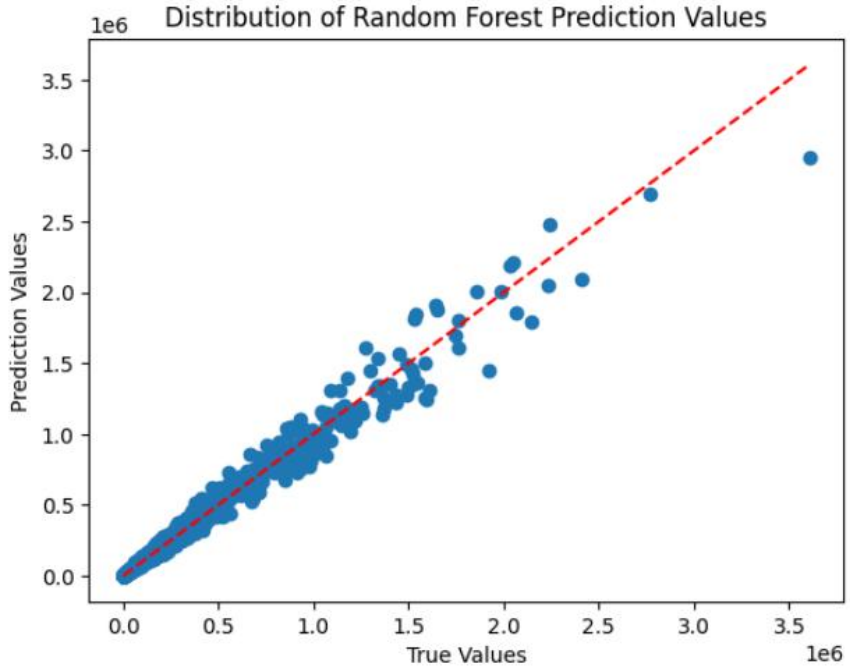

Fig. S20 Distribution of Random Forest prediction values.

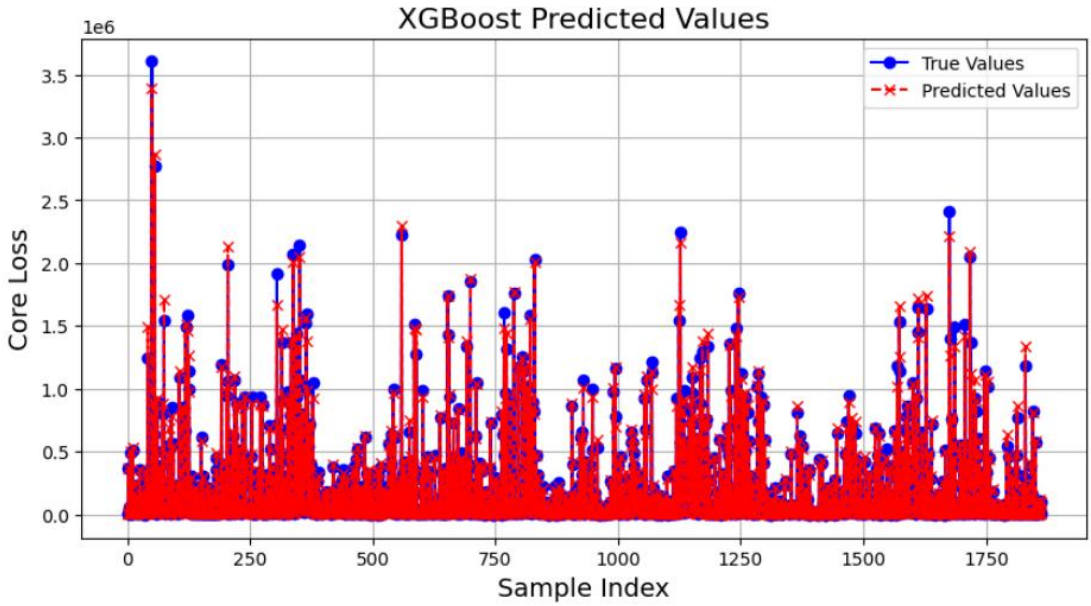

Fig. S21 Comparison between the predicted results of the XGBoost and the actual values.

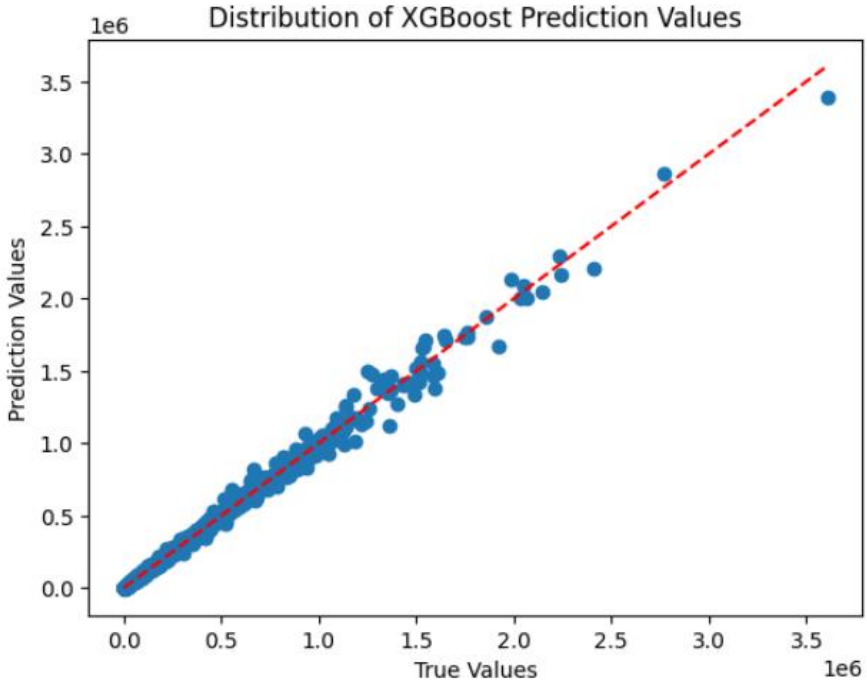

Fig. S22 Distribution of XGBoost prediction values.

6. Prediction results of deep learning models

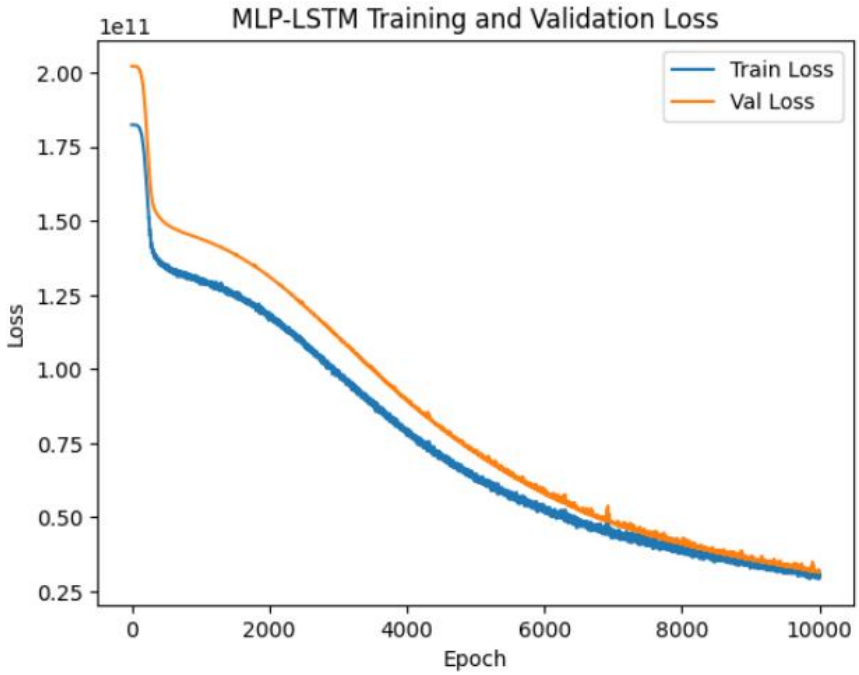

Fig. S23 MLP-LSTM training and validation loss.

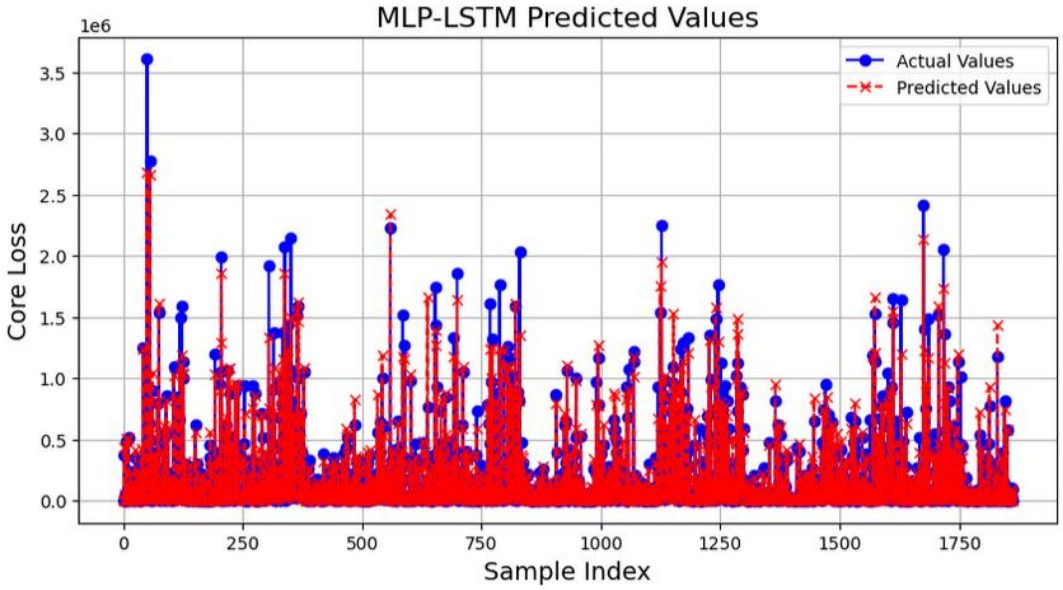

Fig. S24 Comparison between the predicted results of the MLP-LSTM and the actual values.

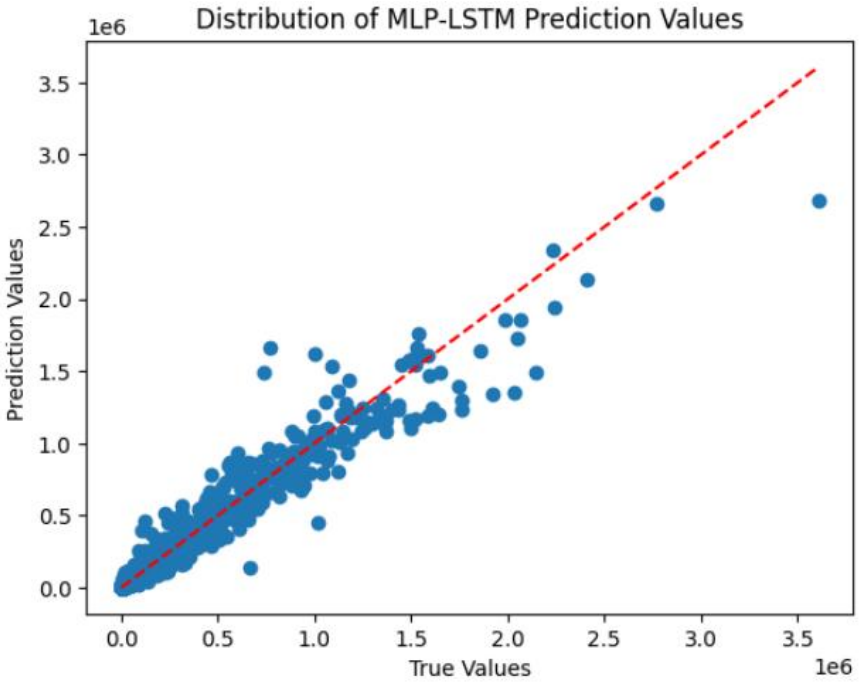

Fig. S25 Distribution of MLP-LSTM prediction values.

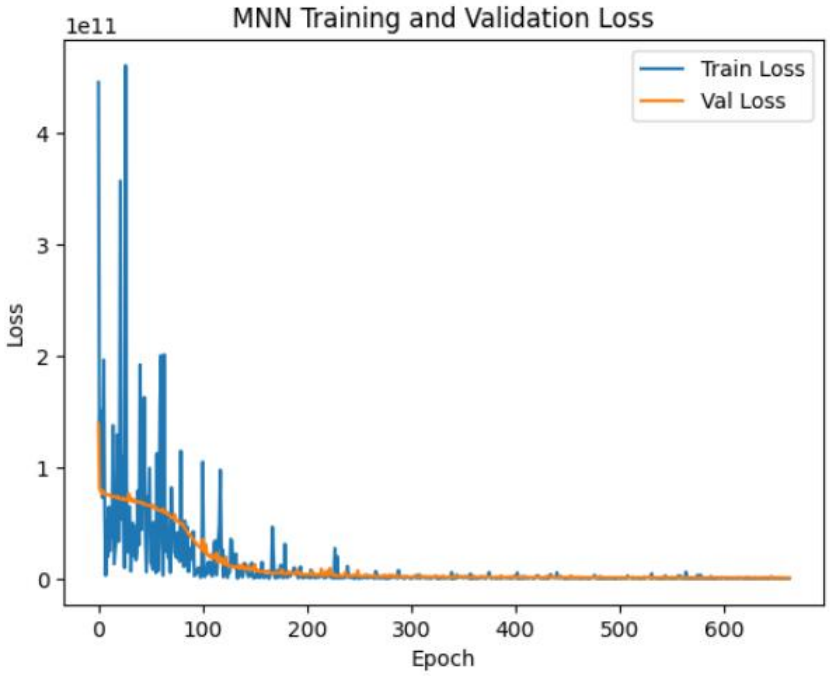

Fig. S26 MNN training and validation loss.

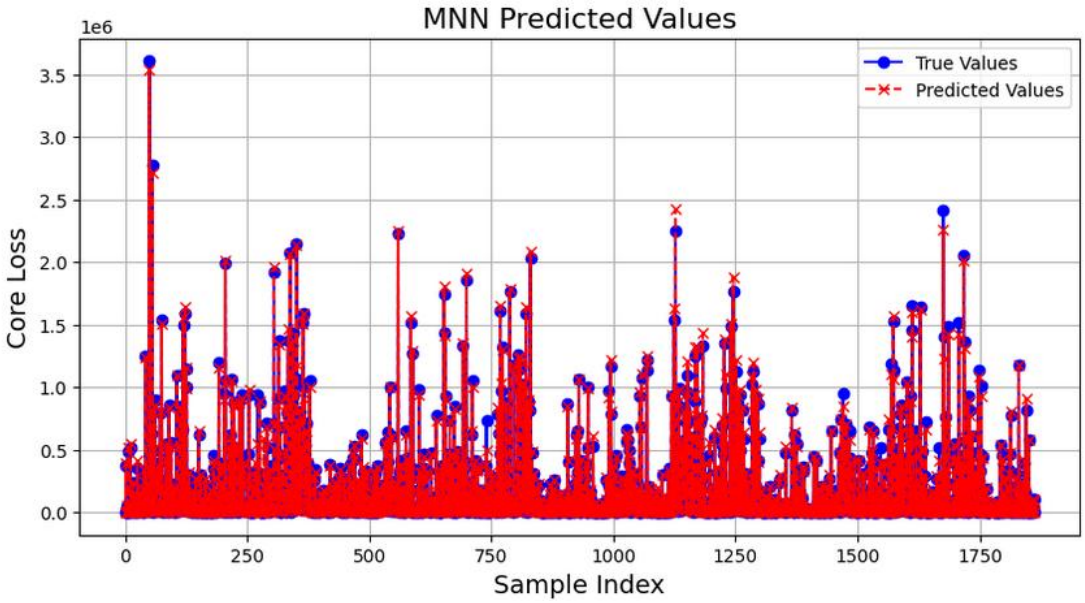

Fig. S27 Comparison between the predicted results of the MNN and the actual values.

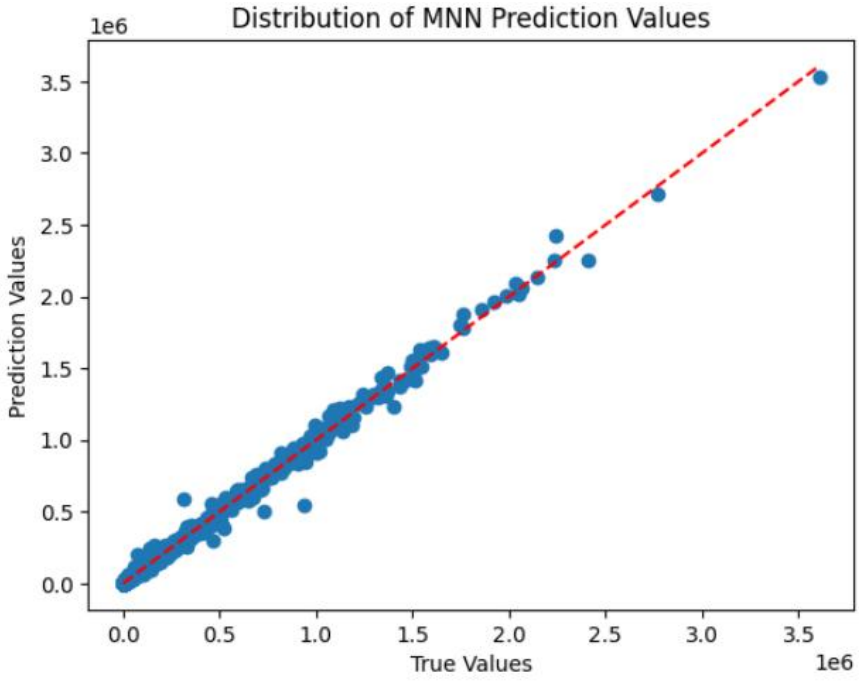

Fig. S28 Distribution of MNN prediction values.

7. Prediction results of all models

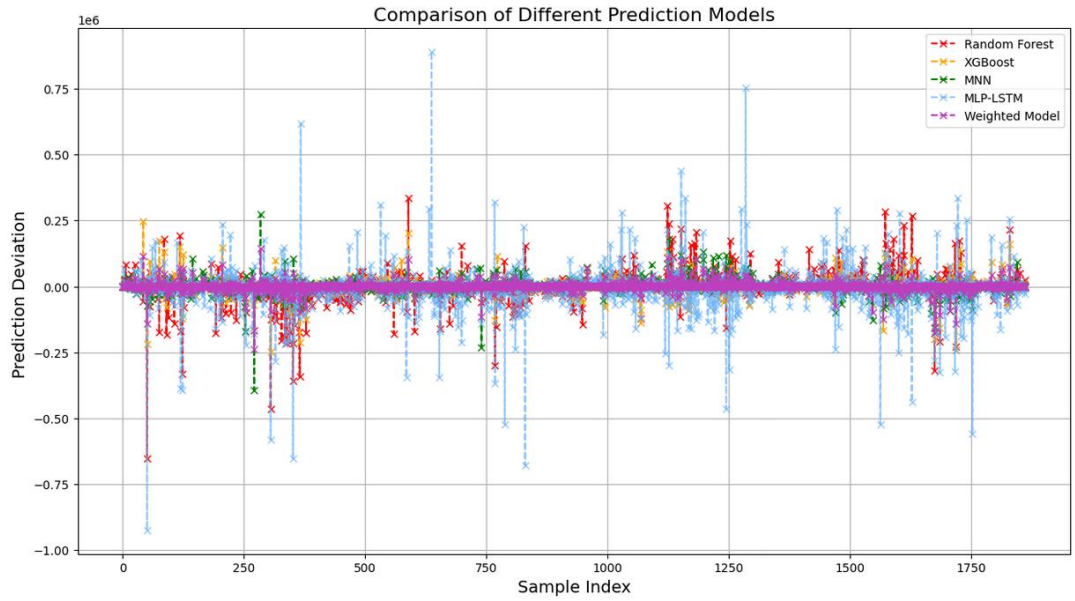

Fig. S29 Residual between predicted and actual values of all models.

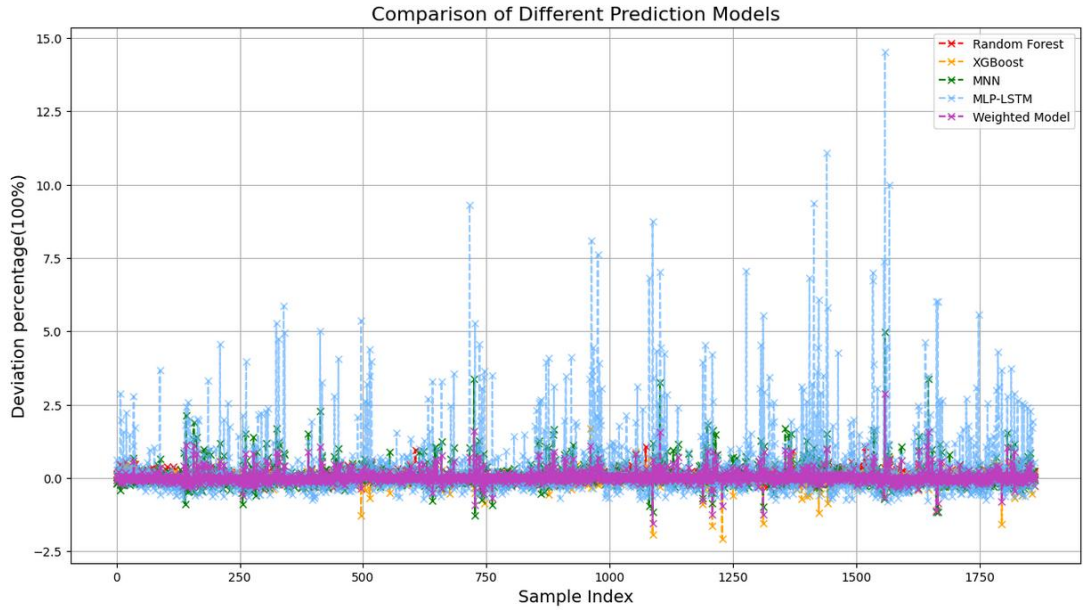

Fig. S30 Percentage of residual between predicted and actual values of all models.